

## Oscillatory Exchange Bias due to an Antiferromagnet with Incommensurate Spin-Density Waves

F. Y. Yang and C. L. Chien

*Department of Physics and Astronomy, The Johns Hopkins University, Baltimore, Maryland 21218*

(Received 31 October 2002; published 9 April 2003)

Oscillatory exchange bias in both magnitude and in sign has been observed in epitaxial (100)Cr/Ni<sub>81</sub>Fe<sub>19</sub> bilayers due to the incommensurate spin-density waves in antiferromagnetic (100)Cr layers. Salient effects due to the spin-flip transition between longitudinal and transverse spin-density waves as well as that of expanding wavelength have been observed.

DOI: 10.1103/PhysRevLett.90.147201

PACS numbers: 75.70.-i, 68.55.-a, 75.25.+z, 75.30.-m

Chromium (Cr) metal exhibits a host of interesting properties, among them, its unique antiferromagnetic (AF) properties. Unlike the well-known AFs with localized moments (e.g., MnF<sub>2</sub>, and CoO) that order into specific spin structures, Cr is an itinerant AF with an incommensurate spin-density wave (SDW) ordering below the Néel temperature  $T_N$ , which for bulk Cr is 311 K. Neutron and x-ray scattering have revealed many fascinating aspects of the SDW in Cr [1–3]. In bulk Cr, the wave vector  $Q_{SDW}$  of the SDW propagates along the {100} directions in the crystal. The magnitude of the magnetic moments along  $Q_{SDW}$  is not constant but sinusoidally modulated with a SDW wavelength  $\Lambda$ , which depends on temperature  $T$ . Furthermore, there are both longitudinal and transverse SDW, where the magnetic moments lie parallel and perpendicular to  $Q_{SDW}$ , respectively. In bulk Cr, transverse SDW exists at  $T$  larger than the spin-flip (SF) transition  $T_{SF} = 123$  K. Below  $T_{SF}$ , the SDW changes from transverse to longitudinal and the moments become parallel to  $Q_{SDW}$ . Very recently, AF domains in bulk single-crystal Cr have also been observed using x-ray microdiffraction [4]. The antiferromagnetic SDW ordering notwithstanding, Cr has also been featured prominently in magnetic nanostructures. Oscillatory interlayer coupling has been observed in Fe/Cr multilayers, in which the sign of the coupling oscillates as the thickness of the intervening Cr layer is varied. The giant magnetoresistance effect was first discovered in antiferromagnetically coupled Fe/Cr multilayers [5–7].

The exchange bias phenomenon between an AF and a ferromagnet (FM) has also captured intense interest because of its intriguing physics and the central role in spin-valve based devices [8,9]. At the interface of a FM and an AF with uncompensated AF moments, the net AF moments at the interface will generate a bias magnetic field and the hysteresis loop of the FM will be shifted away from the origin. It has been generally recognized that the understanding of exchange bias hinges on the AF spin structure and its interaction with the FM layer. To date, virtually all the exchange-biased systems incorporate only AF layers with localized moments (e.g., CoO, FeMn, IrMn, and MnF<sub>2</sub>, etc.). The rich features of the

AF spin structure of Cr provide a unique medium for studying exchange bias. In this Letter, we report the observation of oscillatory exchange bias in epitaxial (100)Cr/FM bilayers, through which we have revealed the effects of incommensurate SDW antiferromagnetic ordering on exchange bias.

Neutron scattering shows that while  $Q_{SDW}$  propagates along the {100} directions in bulk Cr, the  $Q_{SDW}$  is oriented perpendicular to the film plane in thin (100)Cr layers [10,11]. It is therefore essential to fabricate epitaxial (100)Cr thin films to be exchange-coupled to a soft ferromagnet, for which permalloy = Py = Ni<sub>81</sub>Fe<sub>19</sub> has been used. We have made epitaxial (100)Cr/Py bilayers using magnetron sputtering with a base pressure better than  $7 \times 10^{-8}$  Torr in the sequence of (100)MgO/(100)Cr(179 Å)/(100)Au(500 Å)/(100)Cr( $t_{Cr}$ )/Py(100 Å) as shown in Fig. 1(a). The first (100)Cr(179 Å) layer on the (100)MgO substrate serves as the buffer layer for (100)Au(500 Å), which acts as the buffer layer for (100)Cr( $t_{Cr}$ ). Because the lattice constants  $a_{fcc}$  for Au and  $\sqrt{2}a_{bcc}$  for Cr are within 0.003%, the second (100)Cr( $t_{Cr}$ ) layer so produced has little strains, which is important for the study of incommensurate SDW in Cr [3,12]. The (100)Cr(179 Å)/(100)Au(500 Å) buffer layers were grown on a (100)MgO substrate at a substrate temperature of  $T_S = 500^\circ\text{C}$ , followed by the growth of (100)Cr( $t_{Cr}$ )/Py(100 Å) at  $T_S = 150^\circ\text{C}$  with the deposition rates of 1.1 Å/sec for Cr and 1.4 Å/sec for Au. Because of the thick Au layer, only the upper (100)Cr( $t_{Cr}$ ) layer is exchange-coupled to the Py layer. A number of samples have been made where only  $t_{Cr}$  of the upper (100)Cr( $t_{Cr}$ ) layer has been varied from 75 to 448 Å.

The epitaxy of the various layers has been established by x-ray diffraction. The  $\theta/2\theta$  x-ray scan of one example shows only the (200) and (400) peaks of MgO, Au, and Cr, as shown in Fig. 1(c). The pole figures of the off-axis Au(220), Cr(110), and MgO(220) peaks exhibit fourfold symmetry as shown in Fig. 1(d). The 45° rotation of the four-spot patterns among Au(220), Cr(110), and MgO(220) established the epitaxial relationship of the three crystal structures as MgO[001] || Cr[011] || Au[001]

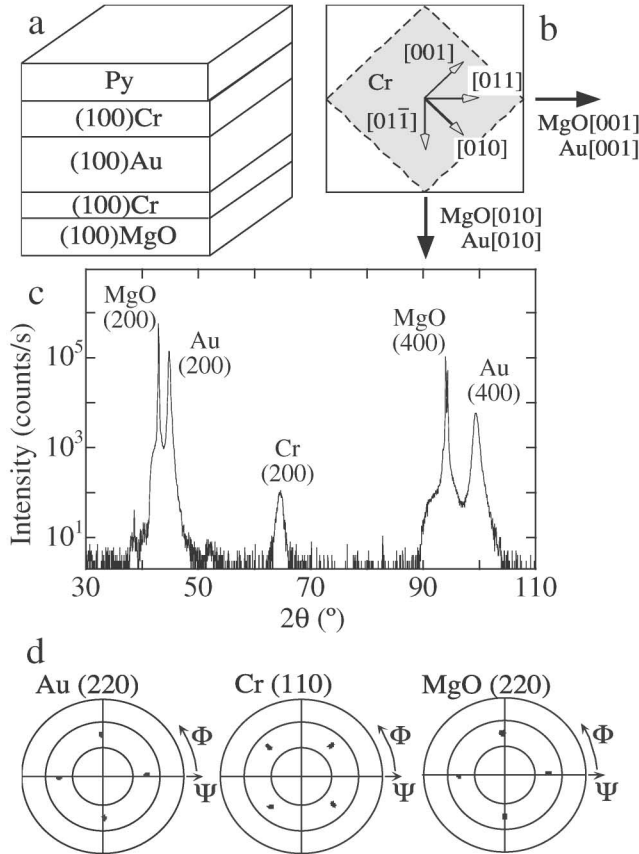


FIG. 1. (a) Layered structure of epitaxial (100)MgO/(100)Cr(179 Å)/(100)Au(500 Å)/(100)Cr( $t_{Cr}$ )/Py(100 Å), (b) epitaxial relation among (100) MgO, Au, and Cr, (c) x-ray  $\theta/2\theta$  diffraction scan of the sample with  $t_{Cr} = 179$  Å showing only the (200) and (400) peaks of MgO, Cr, and Au, and (d) pole figures of Au(220), Cr(110), and MgO(220) confirming the epitaxial relationship shown in (b).

as shown in Fig. 1(b). The rocking curve of the Cr(200) peak gives a full width at half maximum of  $1.1^\circ$  for the 179 Å Cr layer.

The magnetic properties of the essential (100)Cr( $t_{Cr}$ )/Py(100 Å) have been studied by a high-resolution (0.01 Oe) vibrating sample magnetometer at  $T \geq 100$  K and a superconducting quantum interference device (SQUID) magnetometer at lower temperatures for some of the samples. To establish exchange bias, we field cooled (FC) the (100)Cr/Py samples in a magnetic field ( $H_{FC}$ ) of 1.5 T parallel to the [001] axis of Cr from 373 K to low temperatures and measured the hysteresis loops along the same axis.

We have observed exchange bias in all the (100)Cr( $t_{Cr}$ )/Py(100 Å) samples with  $75 \text{ \AA} \leq t_{Cr} \leq 448 \text{ \AA}$ . Representative hysteresis loops of (100)Cr(448 Å)/Py(100 Å) from 25 to 350 K are shown in Fig. 2. Two characteristic fields can be determined from the hysteresis loops,  $H_C^-$  and  $H_C^+$ , where  $H_C^-$  is the switching field at which  $M$  becomes zero as  $H$  was swept from positive to negative and  $H_C^+$  is the switching field as  $H$  was swept back to positive. The coercivity  $H_C = (H_C^+ - H_C^-)/2$  decreases monotonically

with increasing temperature as expected. However, unlike all the other exchange-biased systems, the exchange bias field  $H_E = (H_C^+ + H_C^-)/2$  does not vary monotonically with temperature. It is clear from Fig. 2 that while the values of  $H_E$  at 115 and 225 K are substantial and negative,  $H_E$  is nearly zero at 25 and at 200 K. The temperature dependence of  $H_E$  for  $t_{Cr} = 448$  Å is not monotonic but *oscillatory* as shown in Fig. 3(a). This is the first time that oscillatory behavior of  $H_E$  has been observed in any exchange-biased system.

Samples of (100)Cr( $t_{Cr}$ )/Py(100 Å) with other Cr layer thicknesses show a similar behavior as shown in Fig. 3(a), indicating that the oscillatory exchange bias is a general behavior of (100)Cr( $t_{Cr}$ )/Py. However, while the prominent peak of  $H_E$  is at 115 K for the sample with  $t_{Cr} = 448$  Å, its location occurs at about 50 K for  $t_{Cr} = 179$  Å. This indicates that the location of the prominent peak shifts to lower temperatures for samples with smaller  $t_{Cr}$ . The temperature at which  $H_E$  vanishes is known as the blocking temperature  $T_B$ , whose value is often close to the  $T_N$  of the antiferromagnet (e.g., in CoO) if field cooling commences at  $T > T_N$ . For AF with small layer thickness, the values of  $T_N$  and that of  $T_B$  are depressed

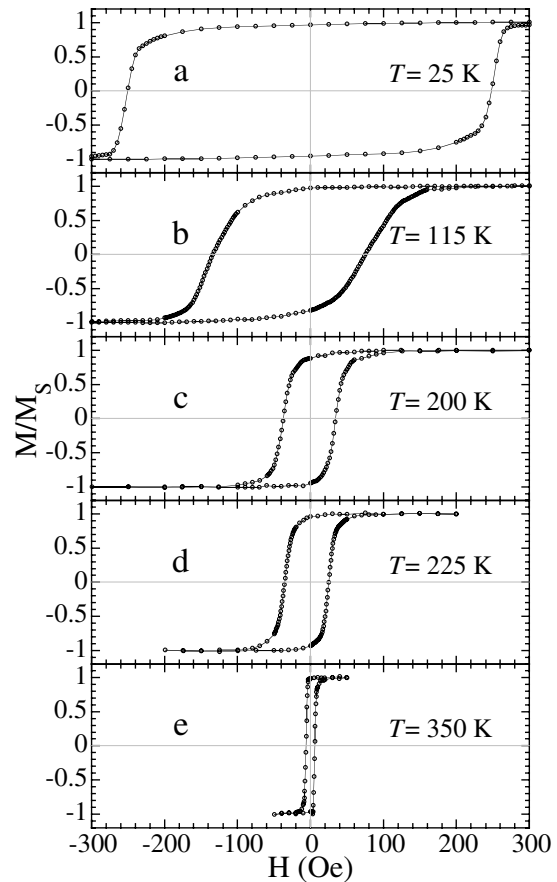


FIG. 2. Hysteresis loops of a (100)Cr(448 Å)/Py(100 Å) bilayer at (a) 25 K, (b) 115 K, (c) 200 K, (d) 225 K, and (e) 350 K with exchange bias fields of  $-2$  Oe,  $-28.6$  Oe,  $-1.2$  Oe,  $-4.8$  Oe, and  $0$  Oe, respectively.

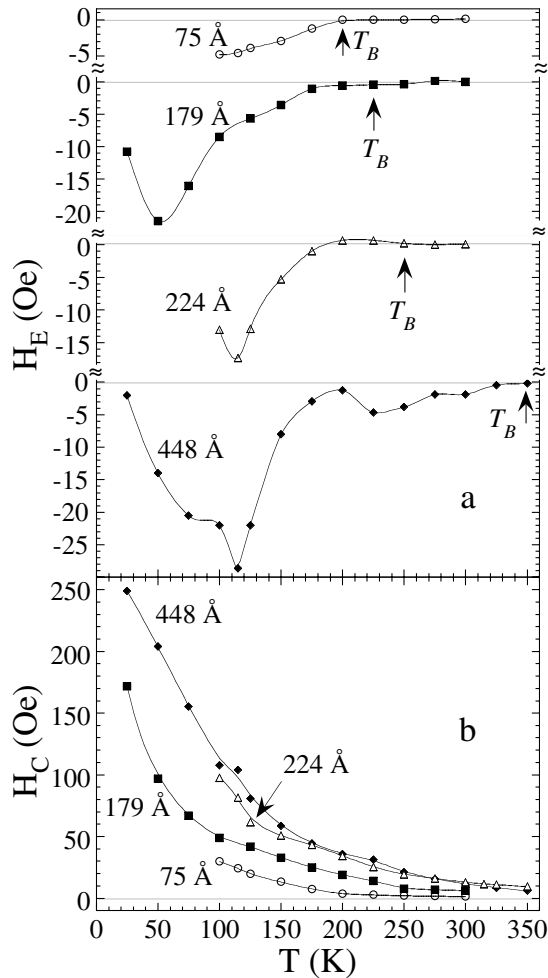


FIG. 3. Temperature dependence of (a)  $H_E$  and (b)  $H_C$  for epitaxial  $(100)\text{Cr}(t_{\text{Cr}})/\text{Py}(100 \text{ \AA})$  bilayers with  $t_{\text{Cr}} = 75, 179, 224,$  and  $448 \text{ \AA}$ .

to lower values due to the finite-size scaling effects [13]. For the samples with  $t_{\text{Cr}} = 448 \text{ \AA}$ , we have found that  $T_B \approx 350 \text{ K}$ , which is close to but slightly higher than the value of  $T_N = 311 \text{ K}$  for bulk Cr due to the commensurate AF phase in the film [2,3]. For the samples with  $t_{\text{Cr}} = 224 \text{ \AA}, 179 \text{ \AA},$  and  $75 \text{ \AA}$ ,  $T_B$  is reduced to about  $250 \text{ K}, 225 \text{ K},$  and  $200 \text{ K}$ , respectively, and the latter agrees well with the neutron scattering result for a  $80\text{-\AA}$ -thick Cr [10].

The coercivity  $H_C$  of all the samples decreases monotonically with temperature without an oscillatory behavior and reaches the free FM layer value at  $T_B$  as shown in Fig. 3(b). However, unlike the  $H_C$  in other exchange-biased systems with a quasilinear temperature dependence, the temperature dependence of  $H_C$  is distinctly nonlinear, with a rapid increase below  $T_B$ . It is also noted that the value of  $H_C$  is higher for the sample with a higher  $t_{\text{Cr}}$ . This is opposite to those of all other exchange-biased systems using conventional AFs, where a thinner AF layer generally causes a larger  $H_C$  [14]. It is particularly noteworthy that while the  $H_E$  values of the samples with  $t_{\text{Cr}} = 179$  and  $448 \text{ \AA}$  are negative even when they are

close to zero, in some cases (e.g.,  $t_{\text{Cr}} = 224 \text{ \AA}$ ) the oscillatory  $H_E$  includes values that are *positive* as well. These results suggest that the oscillatory  $H_E$  in  $(100)\text{Cr}(t_{\text{Cr}})/\text{Py}$  intrinsically involves oscillations in *both* magnitude and sign. While the oscillation in magnitude is prevailing, the observation of oscillation in sign requires superior quality samples.

The most fascinating result in  $(100)\text{Cr}(t_{\text{Cr}})/\text{Py}(100 \text{ \AA})$  is the oscillatory exchange bias, which is due to the incommensurate SDW in the thin  $(100)\text{Cr}$  layer as described below. The exchange bias phenomenon is due to the interaction between the FM and AF moments at the FM/AF interface via a Heisenberg-like interaction of  $\vec{S}_{\text{FM}} \cdot \vec{S}_{\text{AF}}$ , where  $\vec{S}_{\text{FM}}$  and  $\vec{S}_{\text{AF}}$  are the spins of the FM and AF moments, respectively. In exchange bias, the essential quantity is  $\vec{M}_{\text{FM}} \cdot \Delta\vec{M}_{\text{AF}}$ , where  $\vec{M}_{\text{FM}}$  is the magnetization of the FM and  $\Delta\vec{M}_{\text{AF}}$  is the net uncompensated magnetization of the AF at the interface as a result of field cooling. The exchange bias depends on the existence of  $\Delta\vec{M}_{\text{AF}}$ , which has been extensively addressed in other AF systems [9]. The exchange bias also depends on the angle between the directions of  $\vec{M}_{\text{FM}}$  and  $\Delta\vec{M}_{\text{AF}}$ , which is revealed in this work. In particular, should  $\Delta\vec{M}_{\text{AF}}$  become perpendicular to  $\vec{M}_{\text{FM}}$ , there would be no exchange bias. When  $\Delta\vec{M}_{\text{AF}}$  and  $\vec{M}_{\text{FM}}$  are in plane, should  $\Delta\vec{M}_{\text{AF}}$  reverse its sign due to the spin structure of the AF, the sign of the exchange bias would likewise be reversed.

The underlying mechanism of the oscillatory exchange bias in  $(100)\text{Cr}/\text{Py}$  is the AF spin structure of the incommensurate SDW in the thin Cr layer, schematically shown in Fig. 4. For bulk Cr, the spin-flip transition occurs at  $T_{\text{SF}} = 123 \text{ K}$ , where the AF spins change from being perpendicular to  $Q_{\text{SDW}}$  (transverse SDW) to being parallel to  $Q_{\text{SDW}}$  (longitudinal SDW) when  $T$  decreases across  $T_{\text{SF}}$ . For  $(100)\text{Cr}(t_{\text{Cr}})$  thin films,  $Q_{\text{SDW}}$  is perpendicular to the film plane [3,15]. After field cooling from above  $T_N$ , the AF spins first form a transverse SDW below  $T_N$  with  $Q_{\text{SDW}}$  perpendicular to the film plane and the net AF moment  $\Delta\vec{M}_{\text{AF}}$  is parallel to the Cr/Py interface. At  $T_{\text{SF}}$ , the AF spins begin to flip from being perpendicular to  $Q_{\text{SDW}}$  to parallel to  $Q_{\text{SDW}}$  (i.e., from being parallel to perpendicular to the FM/AF interface). The prominent peak of  $H_E$  at  $115 \text{ K}$  in the samples with  $t_{\text{Cr}} = 224$  and  $448 \text{ \AA}$  can be readily identified as  $T_{\text{SF}}$ , whose value is slightly lower than  $123 \text{ K}$  for bulk Cr. This transition at  $T_{\text{SF}}$  in exchange-coupled Cr thin films is not abrupt but gradual. At  $25 \text{ K}$ , the interfacial AF moments for  $t_{\text{Cr}} = 448 \text{ \AA}$  become perpendicular to the film plane resulting in a nearly zero exchange bias field because  $\Delta\vec{M}_{\text{AF}}$  is now perpendicular to  $\vec{M}_{\text{FM}}$ . The value of  $T_{\text{SF}}$  decreases from  $115 \text{ K}$  to lower temperatures for samples with thinner  $t_{\text{Cr}}$ , e.g.,  $50 \text{ K}$  for  $t_{\text{Cr}} = 179 \text{ \AA}$ . Below  $T_{\text{SF}}$ , the coercivity shows a rapid increase of coercivity due to the spin-flip transition. A sharp rise in  $H_C$  below  $130 \text{ K}$  has previously been reported in Fe film on bulk  $(100)\text{Cr}$  [16].

The oscillation of  $H_E$  originates from the expanding wavelength  $\Lambda$  of the incommensurate SDW spin structure

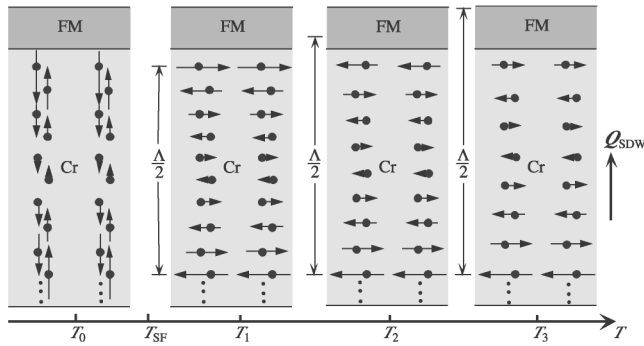


FIG. 4. Schematic representation of the longitudinal SDW below the spin-flip transition temperature  $T_{SF}$ , and three transverse SDW above  $T_{SF}$  with different wavelength  $\Lambda$  at different temperatures.

in Cr. The basic mechanism of the oscillation of  $H_E$  is illustrated in Fig. 4. Because of the expansion of  $\Lambda$  with increasing temperature, the net AF moments at the Cr/FM interface would change its orientation from one direction to the opposite direction at  $T_1$ ,  $T_2$ , and  $T_3$ . This results in a change of sign in  $H_E$  from  $T_1$  to  $T_2$ , and from  $T_2$  to  $T_3$ . Because of the roughness at the interface in actual samples, the sign change of  $H_E$  is often obscured, whereas the oscillation in  $H_E$  is more readily observable. It should be emphasized that the oscillation in  $H_E$  has been observed only in epitaxial Cr layers, but not in polycrystalline Cr, although the latter exhibits exchange bias [17].

It has been well established that the wavelength of the SDW in Cr increases with temperature. For bulk Cr,  $\Lambda$  increases from 60 Å at 10 K to 78 Å at  $T_N = 311$  K [2]. X-ray and neutron scattering showed that  $\Lambda$  is somewhat larger in thin films with  $\Lambda \approx 85$  Å for  $t_{Cr} = 500$  Å at 200 K [15]. While the precise values of  $\Lambda$  in our samples are not known, it is reasonable to assume a similar  $\Lambda \approx 88$  Å in our sample with  $t_{Cr} = 448$  Å at 200 K. The estimated period of oscillation of  $H_E$  in Fig. 3(a) for  $t_{Cr} = 448$  Å is about 75 K above 150 K, suggesting that the SDW AF spins of Cr at the Cr/Py interface have been pushed up across the Cr/Py interface by two atomic layers, i.e., 2.88 Å, from 200 to 275 K. We are aware of no technique that can determine the anchoring point of the SDW at which the Cr spins remain stationary. However, the anchoring point cannot be at the Cr/Py interface or there would be no oscillatory  $H_E$ . If the anchoring point is at the center of the Cr layer,  $\Lambda$  would expand from 88 Å at 200 K to 89 Å at 275 K to account for the observed effect. If the actual anchoring point is closer or away from the center of the Cr layer, the value of  $\Lambda$  at 275 K would be larger or smaller, respectively. For example, if the anchoring point is at 40 Å away from the Cr/Py interface, due to the stronger pinning at the Cr/Py interface,  $\Lambda = 95$  Å at 275 K would be expected. These estimates show that the observed oscillations in exchange bias are consistent with an expanding SDW wavelength.

At temperatures below 150 K, the values of  $\Lambda$  are essentially independent of temperature in both bulk Cr and epitaxial Cr films [15], and indeed no oscillation has been observed. The samples with thin  $t_{Cr}$  (e.g., 75 Å) exhibit no oscillation in  $H_E$  because their blocking temperatures are too low (e.g., 200 K).

In summary, we have observed oscillatory exchange bias field in the magnitude, and in some cases the sign, in epitaxial (100)Cr/Ni<sub>81</sub>Fe<sub>19</sub> bilayers as a function of temperature. The unusual behavior is due to the incommensurate spin-density waves in antiferromagnetic Cr. The prominent peak at about 115 K in the temperature dependence of  $H_E$  is due to the spin-flip transition from transverse to longitudinal SDW, whereas the oscillation of  $H_E$  with temperature is due to the expansion of the SDW wavelength in the Cr layer. The exchange bias measured reveals these aspects of the SDW ordering in the Cr layer. These results also show that exchange bias phenomena depend sensitively on the spin structure of the antiferromagnet, which in the case of Cr, is exceptionally rich.

This work has been supported by NSF Grants No. DMR01-01814 and No. DMR00-80031.

- [1] C.G. Shull and M.K. Wilkinson, Rev. Mod. Phys. **25**, 100 (1953).
- [2] E. Fawcett, Rev. Mod. Phys. **60**, 209 (1988).
- [3] H. Zabel, J. Phys. Condens. Matter **11**, 9303 (1999).
- [4] P.G. Evans, E.D. Isaacs, G. Aeppli, Z. Cai, and B. Lai, Science **295**, 1042 (2002).
- [5] P. Grünberg, R. Schreiber, Y. Pang, M.B. Brodsky, and H. Sowers, Phys. Rev. Lett. **57**, 2442 (1986).
- [6] M.N. Baibich, J.M. Broto, A. Fert, F. Nguyen van Dau, F. Petroff, P. Etienne, G. Creuzet, A. Friederich, and J. Chazeles, Phys. Rev. Lett. **61**, 2472 (1988).
- [7] E.E. Fullerton, K.T. Riggs, C.H. Sowers, S.D. Bader, and A. Berger, Phys. Rev. Lett. **75**, 330 (1995).
- [8] See, e.g., J. Nogus and I.K. Schuller, J. Magn. Magn. Mater. **192**, 203 (1999).
- [9] See, e.g., A.E. Berkowitz and K. Takano, J. Magn. Magn. Mater. **200**, 552 (1999).
- [10] A. Schreyer, C.F. Majkrzak, Th. Zeidler, T. Schmitte, P. Bödeker, K. Theis-Bröhl, A. Abromeit, J.A. Dura, and T. Watanabe, Phys. Rev. Lett. **79**, 4914 (1997).
- [11] P. Bödeker, A. Schreyer, and H. Zabel, Phys. Rev. B **59**, 9408 (1999).
- [12] M.C. Hanf, C. Pirri, J.C. Peruchetti, D. Bolmont, and G. Gewinner, Phys. Rev. B **39**, 1546 (1989).
- [13] T. Ambrose and C.L. Chien, J. Appl. Phys. **83**, 6822 (1998).
- [14] R. Jungblut, R. Coehoorn, M.T. Johnson, J. aan de Stegge, and A. Reinders, J. Appl. Phys. **75**, 6659 (1994).
- [15] P. Sonntag, P. Bödeker, T. Thurston, and H. Zabel, Phys. Rev. B **52**, 7363 (1995).
- [16] A. Berger and H. Hopster, Phys. Rev. Lett. **73**, 193 (1994).
- [17] F.Y. Yang and C.L. Chien, J. Appl. Phys. (to be published).